A complex-screen method for modeling elastic wave reflections

SModl.8

Xiao-Bi Xie and Ru-Shan Wu, University of California, Santa Cruz*

Summary

In this paper. we first give a brief summary of the formulation for calculating reflections from a 3D elastic structure based on a complex-screen method. The incident wave and reflected wave are propagated by using a complex-screen propagator. The reflections are calculated based on local Born approximation. When using a small angle approximation, the backscattering can also be formulated into a screen reflection which has a high computation efficiency and needs relatively small computer memory. As expected from the scattering theory. the forward transmitted waves, like P to P or S to S, are controlled by the P- and S-wave velocity perturbations, while the reflections are controlled by the impedance perturbations. The converted waves are mainly controlled by the density and shear module perturbations.

Numerical examples are given to show the accuracy of the method. For two special cases, the synthetic seismograms obtained with this method are compared with that calculated by elastic finite-difference method. The results show general consistency.

Introduction

The phase screen method and complex screen method have been used to treat the one-way forward propagations for both acoustic and elastic wave problems (e.g. Martin and Flank 1988, Wu and Xie 1993 and Wu 1994), and used as back propagator for seismic wave migration in either acoustic or elastic media (e.g. Stoffa et al. 1900, Wu and Xie 1994). However, many exploration problems show great demand for fast modeling methods to calculate reflections from complex elastic structures, especially for 3D models. Finite-difference and finite-element algorithms are very flexible methods. They can be used for arbitrarily heterogeneous media, but are very time consuming methods. Ray based methods provide high computation efficiency for 3D models but they fail in dealing with complicated 3D volume heterogeneities. In this study, the complex-screen method is extended to deal with the reflections of elastic waves. The interaction between the wave field and the complex screen gives both forward and backward scattered waves. The forward scattered waves, together with the primary wave. construct the transmitted waves. The back-scattered waves give the reflections by the structure. This method preserves the advantages of the complex-screen method. i.e. highefficiency in computation speed and memory, and is a very promising method in modeling reflections from large scale 3D visco-elastic structure.

In the following sections, we first summaize the principle of the method, then give some numerical examples and compare them with results from more accurate finite-difference method.

Expressions for forward and backward scattered wave fields

In this method, the 3D inhomogeneous elastic media is divided into a series of thin slabs perpendicular to the main propagation direction. Once a forward propagated wave incident on one of the slabs. there will be reflected waves and transmitted waves generated by the slab. The transmitted waves rex used as the inputs for the successive slabs. The reflected waves will be back-propagated until they reach the receivers. This iterative process gives both forward and primary reflected waves in a 3D structure.

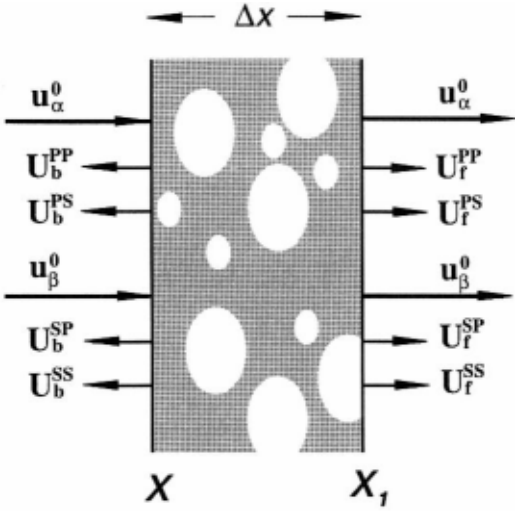

Figure 1. Cartoon showing the primary waves and various scattering waves generated when an incident wave interact with the inhomogeneous slab. Details please see the text.

For a thin slab between x and x_1, consider a primary wave

$$\mathbf{u}^0(x,\mathbf{x}_T) = \frac{1}{4\pi^2}\int d\mathbf{K}_T\,[\mathbf{u}_\alpha^0(x,\mathbf{K}_T) + \mathbf{u}_\beta^0(x,\mathbf{K}_T)]e^{i\mathbf{K}_T\cdot\mathbf{x}_T} \quad (1)$$

composed of P-wave $\mathbf{u}_\alpha^0$ and S-wave $\mathbf{u}_\beta^0$, where $\mathbf{x} = x\,\hat{e}_x + \mathbf{x}_T$, is the position vector and $\mathbf{x}_T$ is the transverse position. Here the wave field has been decomposed into plane waves, and $\mathbf{K}_T$ is the transverse wave number. The interaction between the wavefield and the heterogeneities generates both forward and backward scattered waves. Shown in Figure 1 are primary waves and various types of secondary waves generated by the scattering process. The transmitted wave is composed of primary wave and forward scattered P- and S-waves. At x_1, the forward field can be expressed as

$$\mathbf{u}_f(x_1,\mathbf{x}_T) = \frac{1}{4\pi^2}\int d\mathbf{K}'_T\,[\mathbf{u}_f^P(x_1,\mathbf{K}'_T) + \mathbf{u}_f^S(x_1,\mathbf{K}'_T)]e^{i\mathbf{K}'_T\cdot\mathbf{x}_T} \quad (2)$$

where

$$\mathbf{u}_f^P(x_1,\mathbf{K}'_T) = e^{i\gamma_\alpha \Delta x}\left\{\mathbf{u}_\alpha^0(x,\mathbf{K}'_T) + \frac{1}{4\pi^2}\int d\mathbf{K}_T \left[\mathbf{U}_f^{PP}(\mathbf{K}'_T,\mathbf{K}_T) + \mathbf{U}_f^{SP}(\mathbf{K}'_T,\mathbf{K}_T)\right]\right\} \quad (3)$$

$$\mathbf{u}_f^S(x_1,\mathbf{K}'_T) = e^{i\gamma_\beta \Delta x}\left\{\mathbf{u}_\beta^0(x,\mathbf{K}'_T) + \frac{1}{4\pi^2}\int d\mathbf{K}_T \left[\mathbf{U}_f^{SS}(\mathbf{K}'_T,\mathbf{K}_T) + \mathbf{U}_f^{PS}(\mathbf{K}'_T,\mathbf{K}_T)\right]\right\}. \quad (4)$$

The reflected wave is composed of back-scattered P- and S-waves. At x, the reflected wave can be expressed as

$$\mathbf{u}_b(x,\mathbf{x}_T) = \frac{1}{4\pi^2}\int d\mathbf{K}'_T [\mathbf{u}_b^P(x,\mathbf{K}'_T) + \mathbf{u}_b^S(x,\mathbf{K}'_T)] e^{i\mathbf{K}'_T\cdot\mathbf{x}_T} \quad (5)$$

where

$$\mathbf{u}_b^P(x,\mathbf{K}'_T) = \frac{1}{4\pi^2}\int d\mathbf{K}_T \, X\left[\mathbf{U}_b^{PP}(\mathbf{K}'_T,\mathbf{K}_T) + \mathbf{U}_b^{SP}(\mathbf{K}'_T,\mathbf{K}_T)\right] \quad (6)$$

$$\mathbf{u}_b^S(x,\mathbf{K}'_T) = \frac{1}{4\pi^2}\int d\mathbf{K}_T \, X\left[\mathbf{U}_b^{SS}(\mathbf{K}'_T,\mathbf{K}_T) + \mathbf{U}_b^{PS}(\mathbf{K}'_T,\mathbf{K}_T)\right] \quad (7)$$

In equations (2) to (7), U denotes scattered waves. The subscripts *f* and b denote forward and backward scatterings, respectively and superscripts *PP*, *PS*, *SP*, *SS* indicate the scattering between different wave types.

Under the small angle approximation the forward scattered waves can be derived as

$$\mathbf{U}_f^{PP}(\mathbf{K}'_T,\mathbf{K}_T) \approx -ik_\alpha \Delta x \hat{k}'_\alpha u_\alpha^0(\mathbf{K}_T) \times \frac{\delta\alpha(\tilde{\mathbf{K}}_T)}{\alpha_0}\eta_{fpp}(\Delta x) \quad (8)$$

$$\mathbf{U}_f^{PS}(\mathbf{K}'_T,\mathbf{K}_T) \approx -ik_\beta \Delta x \, u_\alpha^0(\mathbf{K}_T)[\hat{k}_\alpha - \hat{k}'_\beta(\hat{k}_\alpha\cdot\hat{k}'_\beta)] \times\left[\left(\frac{\beta_0}{\alpha_0}-\frac{1}{2}\right)\frac{\delta\rho(\tilde{\mathbf{K}}_T)}{\rho_0} + 2\left(\frac{\beta_0}{\alpha_0}\right)\frac{\delta\beta(\tilde{\mathbf{K}}_T)}{\beta_0}\right]\eta_{fps}(\Delta x) \quad (9)$$

$$\mathbf{U}_f^{SP}(\mathbf{K}'_T,\mathbf{K}_T) \approx -ik_\alpha \Delta x (\mathbf{u}_\beta^0(\mathbf{K}_T)\cdot\hat{k}'_\alpha)\hat{k}'_\alpha \times\left[\left(\frac{\beta_0}{\alpha_0}-\frac{1}{2}\right)\frac{\delta\rho(\tilde{\mathbf{K}}_T)}{\rho_0} + 2\left(\frac{\beta_0}{\alpha_0}\right)\frac{\delta\beta(\tilde{\mathbf{K}}_T)}{\beta_0}\right]\eta_{fsp}(\Delta x) \quad (10)$$

$$\mathbf{U}_f^{SS}(\mathbf{K}'_T,\mathbf{K}_T) \approx -ik_\beta \Delta x \, [\mathbf{u}_\beta^0(\mathbf{K}_T) - \hat{k}'_\beta(\mathbf{u}_\beta^0(\mathbf{K}_T)\cdot\hat{k}'_\beta)]\frac{\delta\beta(\tilde{\mathbf{K}}_T)}{\beta_0}\eta_{fss}(\Delta x) \quad (11)$$

and the backward scattered waves can be derived as

$$\mathbf{U}_b^{PP}(\mathbf{K}'_T,\mathbf{K}_T) \approx ik_\alpha \Delta x \, \hat{k}'_\alpha u_\alpha^0(\mathbf{K}_T) \times \frac{\delta Z_\alpha(\tilde{\mathbf{K}}_T)}{Z_0}\eta_{bpp}(\Delta x) \quad (12)$$

$$\mathbf{U}_b^{PS}(\mathbf{K}'_T,\mathbf{K}_T) \approx -ik_\beta \Delta x \, u_\alpha^0(\mathbf{K}_T)[\hat{k}_\alpha - \hat{k}'_\beta(\hat{k}_\alpha\cdot\hat{k}'_\beta)] \times\left[\left(\frac{\beta_0}{\alpha_0}+\frac{1}{2}\right)\frac{\delta\rho(\tilde{\mathbf{K}}_T)}{\rho_0} + 2\left(\frac{\beta_0}{\alpha_0}\right)\frac{\delta\beta(\tilde{\mathbf{K}}_T)}{\beta_0}\right]\eta_{bps}(\Delta x) \quad (13)$$

$$\mathbf{U}_b^{SP}(\mathbf{K}'_T,\mathbf{K}_T) \approx -ik_\alpha \Delta x (\mathbf{u}_\beta^0(\mathbf{K}_T)\cdot\hat{k}'_\alpha)\hat{k}'_\alpha \times\left[\left(\frac{\beta_0}{\alpha_0}+\frac{1}{2}\right)\frac{\delta\rho(\tilde{\mathbf{K}}_T)}{\rho_0} + 2\left(\frac{\beta_0}{\alpha_0}\right)\frac{\delta\beta(\tilde{\mathbf{K}}_T)}{\beta_0}\right]\eta_{bsp}(\Delta x) \quad (14)$$

$$\mathbf{U}_b^{SS}(\mathbf{K}'_T,\mathbf{K}_T) \approx -ik_\beta \Delta x\left[\mathbf{u}_\beta^0(\mathbf{K}_T) - \hat{k}'_\beta(\mathbf{u}_\beta^0(\mathbf{K}_T)\cdot\hat{k}'_\beta)\right]\frac{\delta Z_\beta(\tilde{\mathbf{K}}_T)}{Z_{\beta 0}}\eta_{bss}(\Delta x) \quad (15)$$

In equations (8) to (15), $\mathbf{k}_\alpha$ and $\mathbf{k}_\beta$ are P- and S-wavenumber vectors for incident wave and k', and $\mathbf{k}'_\beta$ are P- and S-wavenumber vectors for scattered wave.

$$\begin{aligned}\mathbf{k}_\alpha &= \gamma_\alpha \hat{e}_x + \mathbf{K}_T\\ \mathrm{kp} &= \gamma_\beta \hat{e}_x + \mathbf{K}_T\\ \mathbf{k}'_\alpha &= \gamma'_\alpha \hat{e}_x + \mathbf{K}'_T\\ \mathrm{k'p} &= \gamma'_\beta \hat{e}_x + \mathbf{K}'_T\,.\end{aligned} \quad (16)$$

where γ_α, γ_β, γ'_α and γ'_β are longitudinal wavenumbers along x-direction. $\delta\alpha(\mathbf{K}_T)$, $\delta\beta(\mathbf{K}_T)$ and $\delta\rho(\mathbf{K}_T)$ are 2D Fourier transforms of the P- and S-wave velocity and density perturbations of the slab. $Z_\alpha(\mathbf{K}_T)$ and $Z_\beta(\mathbf{K}_T)$ are 2D spectra of P- and S-wave impedance perturbations, respectively. $\tilde{\mathbf{K}}_T = \mathbf{K}'_T - \mathbf{K}_T$ is the exchange vector. The spectrum modulation factors

$$\begin{aligned}\eta_{fpp}(\Delta x) &= 1\\ \eta_{fps}(\Delta x) &= sinc((k_\beta - k_\alpha)\Delta x/2)e^{-i(k_\beta - k_\alpha)\Delta x/2}\\ \eta_{fsp}(\Delta x) &= \eta_{fps}^*(\Delta x)\\ \eta_{fss}(\Delta x) &= 1\\ \eta_{bpp}(\mathrm{Ax}) &= sine(k_\alpha \Delta x)e^{ik_\alpha \Delta x}\\ \eta_{bps}(\Delta x) &= sinc((k_\beta + k_\alpha)\Delta x/2)e^{i(k_\beta + k_\alpha)\Delta x/2}\\ \eta_{bsp}(\Delta x) &= \eta_{bps}(\Delta x)\\ \eta_{bss}(Ax) &= sinc(k_\beta \Delta x)e^{ik_\beta \Delta x}\end{aligned} \quad (17)$$

where $sinc(x) = sin(x)/x$ and Δx is the thickness of the slab.

Equations (1) to (7) construct an iterative algorithm that can either be used to calculate reflections or used as propagator to propagate transmitted waves. Under the small angle approximation, the scattered waves calculated from equations (8) to (15) are convolutions between the incident wave fields and the medium parameters in wavenumber domain. The convolutions can be performed in spatial domain by simple multiplications. By using dual-domain technique shutling between spatial and wavenumber domains, the propagation can be very efficient.

Numerical Examples

The method and numerical code presented in this study is for three dimensions. However, to compare the results with that calculated by 2D elastic finite-difference

code. we calculate synthetic seismograms for 2D models. Figure 2 shows two velocity models used to calculate synthetic seismograms. For these models, the parameters for the background media arc a = 3500m/s. p = 2050m/s and p = *2200kg/m*^{3}. The inclusions have a 5% perturbation for both P- and S-wave velocities. The receiver arrays are indicated by small solid squares. The maximum frequency calculated is 125 Hz. To compare with the finite-difference results, the synthetic seismograms are convolved with a Gaussian derivative source time function having a dominant frequency of 30 Hz. To reduce the contaminations from artificial boundaries, a wavenumber domain taper is used.

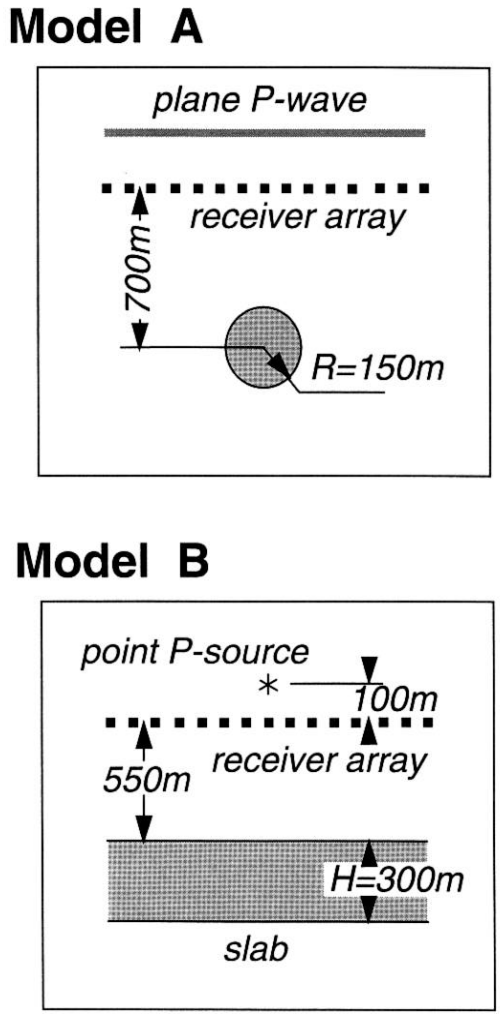

Figure 2. Two dimensional models used to compare the results from complex-screen method and finite-difference method. Model A is a solid cylinder buried in a homogeneous background. A plane P-wave illuminates the model. Model B is a slab in a homogeneous background. The source is a P-wave line source. The receiver arrays are marked with small solid squares. For both models. the parameters for the background media are a = 3500mis. β = 2050m/s and p = *2200kg/m*^{3}. *The inclusions* have a 5% perturbatian for both P- and S-wave velocities.

Model A is a solid cylinder buried in a background medium. The diameter of the cylinder is 300m. A plane P-wave is incident on the cylinder. The geometry of the source and model is shown in Figure 2a. Figure 3 gives the synthetic seismograms from a receiver array 700m away from the center of the cylinder. The synthetics marked with SCREEN is from complex-screen method while marked with FD is from finite-difference method. The upper panel is for y-component (transverse component) and the lower pane, is for x-component (longitudinal component). Shown in the figure are two P-arrivals and two S-arrivals which are reflections from both the upper and lower boundaries of the cylinder. The results show general consistency in both amplitude and arrival time. Considering that the receiver array is only 550m from the border of the cylinder, the profile span a rather wide scattering angle. That means even a small angle approximation can give satisfactory results.

The second example is for P-wave from a line source incident on a homogeneous slab. The geometry of the source and model are shown in Figure 2b. The slab has a thickness of 300 m. The receiver array is 550 m away from the slab. The synthetic seismograms are shown in Figure 4.

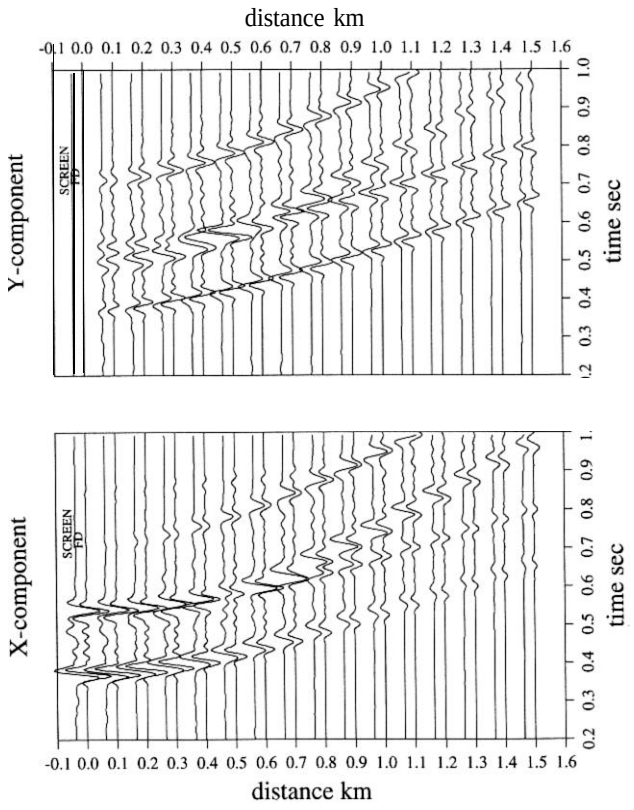

Figure 3. Camparison between synthetic seismograms calculatd for mode, A. The synthetics marked with SCREEN is from complex-screen method and marked with FD is from finite-difference method . The upper panel is for y-component (transverse component) and the lower panel is for x-component (longitudinal component). The results show genera, consistency in both amplitude and arrival time.

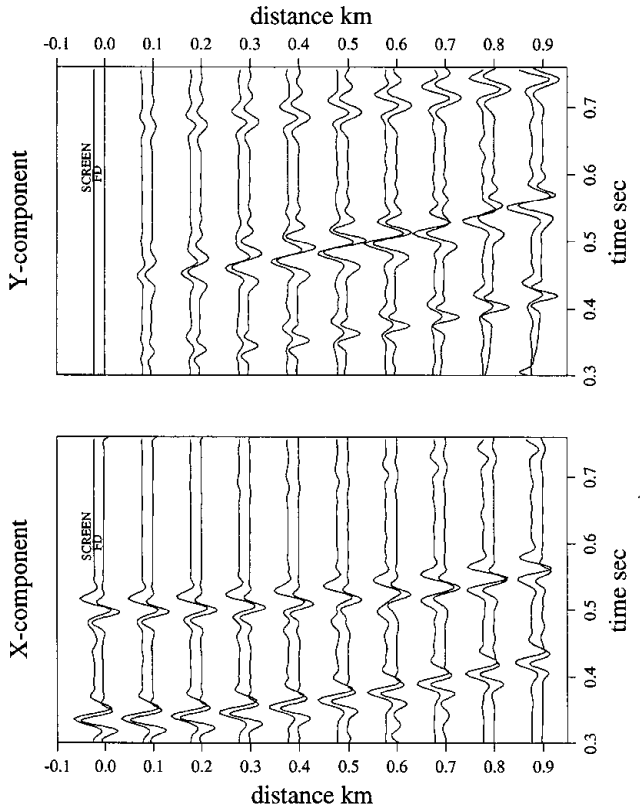

Figure 4. Similar to that in Figure 3 except the synthetics are calculated for model B.

The reflections from both sides of the slab show hyperbolic travel time curves. Resulted from the reversed impedance jump, the polarizations from two sides of the slab are reversed. Similar to that for model A, The results show general consistency

Discussions and Conclusion

A complex-screen method for calculating the reflections of elastic wave from a complex 3D structure is formulated. Since the method needs store only one layer of wave field and model parameters, it requires relatively small computer memory and makes it a promising candidate to do large scale 3D elastic wave reflection modeling. Numerical experiments show that the reflected waves calculated with screen method is consistent with that calculated by finite-difference method.

For forward propagation, the scattered waves sense only the large scale structure along the propagation direction. Therefore the screen method can march with large steps and gives a high computation efficiency. However, for back-scattering, the scattered waves are sensitive to small scale structures. This implies that the screen method has to march with small steps when calculate reflections. A feasible way to overcome this problem is upgrade the forward propagated wave with large steps while calculate the reflections with small steps. Since the forward propagated wave changes slowly, it is expected that this approximation will not introduce big errors while greatly increase the computation efficiency.

Acknowledgement This work is supported partly by the Airforce Office of Scientific Research through contract F49620-95 l-0028 administered by the Phillips Laboratory of the Air Force and partly by a grant from the Los Alamos National Laboratory Institutional Supported Research Program, under the auspices of the United States Department of Energy.

References

Martin, J.M., and S.M. Flatte, 1988, Intensity images and statistics from numerical simulation of wave propagation in 2-D random media, Appl. Opt., 17, 2111-2126.

Stoffa, P.L., J.T. Fokkema, R.M.D. Freire, and W.P. Kessinger, 1990, Split-step Fourier Migration, Geophysics, 55, 410-421.

Wu, R.S., 1994, Wide-angle elastic wave one-way propagation in heterogeneous media and an elastic wave complex-screen method, J. Geophys. Res., 99, 751-766.

Wu, R.S., and X.B. Xie, 1993, A complex-screen method for elastic wave one-way propagation in heterogeneous media, Expanded Abstracts of the 3rd international congress of the Brazilian Geophysical Society.

Wu, R.S. and X.B., Xie, 1994, Multi-screen backpropagator for fast 3D elastic prestack migration, in: Mathematical Methods in Geophysical Imaging II, SPIE Proceedings Series, Vol 2301, 18 1- 193.